frontiers | Frontiers in Neurology

TYPE Brief Research Report
PUBLISHED 24 August 2023
DOI 10.3389/fneur.2023.1210811

Check for updates

OPEN ACCESS

EDITED BY
Marcelo M. Valença,
Federal University of Pernambuco, Brazil

REVIEWED BY
Nikoletta Szabó,
University of Szeged, Hungary
Jan Dirk Blom,
Parnassia Psychiatric Institute, Netherlands

*CORRESPONDENCE
Valentina Mancini
✉ valentina.mancini@unige.ch

RECEIVED 23 April 2023
ACCEPTED 09 August 2023
PUBLISHED 24 August 2023

CITATION
Mastria G, Mancini V, Viganò A, Piervincenzi C, Petsas N, Puma M, Giannì C, Pantano P and Di Piero V (2023) Neuroimaging markers of Alice in Wonderland syndrome in patients with migraine with aura.
Front. Neurol. 14:1210811.
doi: 10.3389/fneur.2023.1210811

COPYRIGHT
© 2023 Mastria, Mancini, Viganò, Piervincenzi, Petsas, Puma, Giannì, Pantano and Di Piero. This is an open-access article distributed under the terms of the Creative Commons Attribution License (CC BY). The use, distribution or reproduction in other forums is permitted, provided the original author(s) and the copyright owner(s) are credited and that the original publication in this journal is cited, in accordance with accepted academic practice. No use, distribution or reproduction is permitted which does not comply with these terms.

Neuroimaging markers of Alice in Wonderland syndrome in patients with migraine with aura

Giulio Mastria[1,2], Valentina Mancini[2,3]*, Alessandro Viganò[4], Claudia Piervincenzi[2], Nikolaos Petsas[5], Marta Puma[2], Costanza Giannì[2,6], Patrizia Pantano[2,6] and Vittorio Di Piero[2]

[1]My Space Lab, Department of Clinical Neuroscience, Centre Hospitalier Universitaire Vaudois (CHUV), University of Lausanne, Lausanne, Switzerland, [2]Department of Human Neurosciences, Sapienza University of Rome, Rome, Italy, [3]Developmental Imaging and Psychopathology Laboratory, University of Geneva School of Medicine, Geneva, Switzerland, [4]IRCCS Fondazione Don Carlo Gnocchi, Milan, Italy, [5]Department of Public Health and Infectious Diseases, Sapienza University of Rome, Rome, Italy, [6]IRCCS NEUROMED, Pozzilli, IS, Italy

Background: The Alice in Wonderland syndrome (AIWS) is a transient neurological disturbance characterized by sensory distortions most frequently associated with migraine in adults. Some lines of evidence suggest that AIWS and migraine might share common pathophysiological mechanisms, therefore we set out to investigate the common and distinct neurophysiological alterations associated with these conditions in migraineurs.

Methods: We conducted a case–control study acquiring resting-state fMRI data from 12 migraine patients with AIWS, 12 patients with migraine with typical aura (MA) and 24 age-matched healthy controls (HC). We then compared the interictal thalamic seed-to-voxel and ROI-to-ROI cortico-cortical resting-state functional connectivity between the 3 groups.

Results: We found a common pattern of altered thalamic connectivity in MA and AIWS, compared to HC, with more profound and diffuse alterations observed in AIWS. The ROI-to-ROI functional connectivity analysis highlighted an increased connectivity between a lateral occipital region corresponding to area V3 and the posterior part of the superior temporal sulcus (STS) in AIWS, compared to both MA and HC.

Conclusion: The posterior STS is a multisensory integration area, while area V3 is considered the starting point of the cortical spreading depression (CSD), the neural correlate of migraine aura. This interictal hyperconnectivity might increase the probability of the CSD to directly diffuse to the posterior STS or deactivating it, causing the AIWS symptoms during the ictal phase. Taken together, these results suggest that AIWS in migraineurs might be a form of complex migraine aura, characterized by the involvement of associative and multisensory integration areas.

KEYWORDS

Alice in Wonderland syndrome, migraine with atypical aura, migraine with aura, superior temporal sulcus, functional connectivity, thalamus, V3

1. Introduction

Migraine represents the first cause of disability in young individuals and the seventh cause of disability in the global population (1, 2). The wide clinical spectrum of migraine includes not only pain but also transient neurological symptoms such as visual aura that may be temporally associated with the headache phase (3). The Alice in Wonderland Syndrome (AIWS) has been recently added to this spectrum (4–7), with migraine described as the most frequent cause of this condition in adult individuals (8).

AIWS is a transient neurological disturbance causing sensory distortions, with a variable combination of micro- and macropsia (seeing objects smaller or larger), telo- and pelopsia (seeing objects further or closer), macro- and micro-somatognosia (perceiving parts of the own body as bigger or smaller), and slowing in perception of time (8–11). Since it first description by the British neurologist J. Todd (9), AIWS has been linked to several underlying etiologies (8–11), ranging from viral infections, such as Epstein–Barr (12), psychiatric comorbidities, adverse effects of common medications, stroke or brain tumors (13–15). Despite the numerous cases available in the literature (8, 11), little is known about AIWS pathophysiological mechanisms.

Recently, a voxel-based meta-analysis including all cases of AIWS associated with a structural lesion (16–20), showed that lesions in extrastriate visual cortex are those most frequently associated with AIWS with visual symptoms (22). To date, it remains to be elucidated if a similar brain network is implicated in AIWS caused by a non-structural disease (functional AIWS). Overall, available single-case studies in AIWS with functional neuroimaging correlates pointed to a hypoactivation of frontal regions, together with increased activation of associative parietal and occipital cortices (16–20). However, the heterogeneity of the clinical presentation, the underlying etiologies, and the variety of the methods employed to measure brain activity (i.e., fMRI, PET, and SPECT) in these studies prevents from drawing strong conclusions.

Migraine might offer a homogeneous model to investigate functional brain alterations associated with AIWS, and the possibility to compare them with findings of AIWS caused by structural brain lesions. Recent evidences highlighted a strong link between AIWS and migraine (4, 22), with up to 20% of migraine patients in a tertiary referral headache clinic reporting symptoms compatible with AIWS (6). Furthermore, almost all the migraineurs with AIWS had a diagnosis of migraine with aura and a temporal concurrence of migraine attacks and AIWS episodes, suggesting that AIWS associated with migraine might be a form of complex aura with high-level cortical dysfunction (6, 23).

Resting-state functional MRI (rs-fMRI) studies in patients with migraine with aura have highlighted a wide range of abnormalities in the interictal and ictal phases, including increased functional connectivity within the visual networks and other regions involved in visual processing (24, 25), although this finding was not confirmed by other studies [for reviews, see Skorobogatykh et al. (26), Chong et al. (27)]. The severity of these alterations has been also associated with the complexity of the migraine aura (28). Moreover, several studies have demonstrated abnormal functional connectivity (FC) between the posterior thalamus, visual cortex and precuneus in migraineurs (29–31) and more severe alterations of thalamic microstructure and structural thalamo-cortical connectivity in subjects with complex migraine aura (28).

In a previous study (21), we compared functional connectivity *within* resting-state networks in AIWS and in patients with typical migraine aura. Alterations related to AIWS were mainly found in lateral and medial visual network. However, AIWS symptoms include both visual and somatosensory distortions that can potentially originate from impairments in the integration of multisensory stimuli, i.e., visual and somatosensory information about the structure of the body and its relationship with the environment. Therefore, with our previous approach it was not possible to identify alterations in inter-regional connectivity *between* brain networks (e.g., visual and somato-motor network), which are possibly implicated in AIWS manifestations.

The aim of the present study was to pinpoint neuroimaging-measured markers of functional AIWS related to migraine, exploring the connectivity between brain regions, regardless of their belonging to specific networks. We compared ROI based cortico-cortical and thalamic seed-to-voxel FC of a group of patients with migraine experiencing AIWS episodes in the context of migraine attacks, a group of migraineurs with typical aura (MA; ICHD-3 1.2.1), and a group of healthy controls (HC). We searched for common and distinct neurophysiological alterations in AIWS and MA, to clarify the specific mechanisms underlying AIWS in this population and their possible relationship with typical migraine aura.

2. Materials and methods

2.1. Participants

We recruited consecutive patients with migraine with aura experiencing AIWS in the context of migraine attacks (AIWS) and sex-matched patients with migraine with typical visual and somatosensory aura (MA) at the Headache Center of Policlinico Umberto I of Rome. Because of the high within-subject aura variability (32), we included patients without a preferred side of aura symptoms. Neuroimaging data were collected during the inter-ictal period according to the migraine diary filled by patients. All patients were naïve for preventive migraine medication prior to image acquisition.

AIWS participants and MA were recruited in the context of a cohort study at the Headache Center aimed at estimating the prevalence of AIWS in patients with migraine by means of an *ad-hoc* questionnaire over a period of 1.5 years (6). No statistical power calculation was conducted before the study and the sample size was based on all the available data. Answers to the questionnaire were validated by trained physicians and additional information about AIWS were collected, including clinical characteristics of AIWS episodes, such as the age of onset and the temporal association between AIWS, migraine and aura (6). Patients with a diagnosis of migraine with aura according to the International Classification of Headache Disorders, 3rd edition (ICHD-3), who experienced at least one episode of AIWS temporally associated with migraine attacks (i.e., from 60 min prior to pain onset to pain resolution) were included in the AIWS group. Patients with a diagnosis of migraine with aura according to the ICHD-3 without AIWS were included in the MA group. A group of sex- and age-matched healthy controls without any significant neurological or systemic disorders was blindly selected among those available from the Human Neurosciences Department archive.

The following exclusion criteria were applied to all the subjects: medically unstable or with hematological, renal, or hepatic dysfunction; history of moderate to severe head injury, stroke, or seizures; alcoholism or drug dependency.

The study was approved by the ethics committee of Policlinico Umberto I (reference: 4839/2018) and was carried out in accordance with the latest Declaration of Helsinki. All participants provided written informed consent to the use of their data for research purpose.

2.2. MRI acquisition

All the images were acquired with a 3 T MAGNETOM Verio scanner (Siemens AG, Erlangen, Germany) with a 12-channel head coil designed for parallel imaging (GRAPPA) at Sapienza University of Rome. A multiplanar T1-weighted localizer image with section orientation parallel to the subcallosal line was acquired at the start of each MRI examination. Noise reduction headphones were used for attenuation of scanner noise. MRI protocol included, in the following order: (1) high-resolution 3D, T1-weighted MPRAGE sequence: TR = 1,900 ms; TE = 2.93 ms; flip angle = 9°; field of view (FOV) = 260 mm; matrix = 256 × 256; 176 sagittal slices 1 mm thick, with no gap, 0.5 mm in-plane resolution; (2) resting state functional MRI (rs-fMRI): repetition time (TR) = 3,000 ms, echo time (TE) = 30 ms, flip angle = 89°, 64 × 64 matrix, 50 contiguous axial slices 3 mm thick, 3 mm in-plane resolution, 140 volumes (before being positioned in the scanner patients were instructed to lie down relaxed and awake with eyes closed); (3) dual turbo spin-echo, proton density (PD) and (4) T2-weighted images (TR = 3,320 ms, TE1 = 10 ms, TE2 = 103 ms, FOV = 220 mm, matrix = 384 × 384, 25 axial slices 4 mm thick, 30% gap), as well as (5) High-resolution 3D, fluid-attenuated inversion recovery (FLAIR) sequence (TR = 6,000 ms, TE = 395 ms, TI = 2,100 ms, FOV = 256 mm, matrix = 256 × 256, 176 sagittal slices 1 mm thick, no gap) were also acquired to exclude concomitant brain lesions.

2.3. Structural images preprocessing

T1-weighted images underwent fully automated image processing with the Connectome mapper v3, a neuroimaging pipeline software combining tools such as Freesurfer v.6, FSL, ANTs, MRtrix3, Dipy and AFNI (33). Structural images preprocessing comprised skull stripping, intensity normalization, reconstruction of internal and external cortical surfaces and parcellation of subcortical brain regions (34) and further parcellation with the Lausanne atlas characterized by identical cortical regions of interest of desired size and location at different scales [from 1 corresponding to the Desikan and Killiany atlas to 5 corresponding to the smallest size (35)]. The ROI-to-ROI FC analysis were conducted using the intermediate scale (scale 3, 216 cortical parcels).

2.4. fMRI images preprocessing

The functional images were preprocessed using SPM12 (Statistical Parametric Mapping, Wellcome Department of Imaging Neuroscience).[1] All the functional images were realigned to the mean image volume with a six-parameter rigid body transformation and the structural scans were then co-registered to the functional mean. The anatomical images were segmented into gray matter, white matter and cerebrospinal fluid (CSF) with the SPM12 *Segmentation* algorithm (36). The resulting images were spatially smoothed using an isotropic Gaussian kernel of 6 mm full width maximum (FWHM) and normalized to the MNI template.

Further steps of preprocessing and FC analyses were carried out using the CONN-fMRI Functional Connectivity toolbox v18[2] (37). Parcellations from the Lausanne atlas based on individual anatomy were imported in *Conn* as subject-specific ROIs. Outlier scans due to head motion were identified using the software *ART*[3] (38) and excluded if the movement of either translational or rotational parameters exceeded 2 mm or 2°. After all these quality control procedures, no subject was excluded from the following analyses.

BOLD signal noise from white matter and CSF was defined and addressed with the Component-based correction (CompCor) method, which models the influence of noise as a voxel-specific combination of multiple noise sources (37, 39). The first 5 principal components of the subject-specific WM- and CSF-mask signals were calculated. Then, the linear effects of the 6 motion parameters estimated during realignment, their temporal derivatives, and the 5 noise components (including physiological artifacts such as cardiac or respiratory rates) were regressed out at each voxel. Furthermore, outliers time-points identified with the software *ART* by using a global-signal z-value threshold of 3 and a subject motion threshold of 0.5 mm were as well scrubbed from the BOLD time-series at each voxel. Finally, the BOLD time-series within each of the seeds was estimated and temporally band-pass filtered with a frequency window of 0.008 to 0.09 Hz.

2.5. Cortico-cortical and whole brain thalamic functional connectivity analyses

The analysis of the whole-brain thalamic FC was conducted on the images normalized in MNI space. We used *a priori* anatomically delineated thalami as seeds (40, 41) and we merged the bilateral thalami since our patients did not showed a preferred side in aura and AIWS symptoms. Seed-to-voxel FC analyses were carried on between the thalami and whole brain.

For the study of the cortico-cortical FC, a ROI-to-ROI FC analysis was carried on between all the ROIs as defined by the Lausanne atlas in the native space of each subject. ROI-to-ROI FC maps were created for each participant, modeling individual-specific covariation between the BOLD activity of each ROI and that of all the other cortical ROIs (37).

2.6. Statistical analyses

In the seed-to voxel analysis, we used a T-contrast to compare AIWS with HC (voxel level threshold: $p < 0.001$, cluster level $p < 0.05$

1 https://www.fil.ion.ucl.ac.uk/spm/software/spm12/
2 https://web.conn-toolbox.org
3 www.nitrc.org/projects/artifact_detect

FDR corrected). We then focused on the resulting clusters of voxels and compared their FC with the thalamus between the three groups using t-tests ($p < 0.05$ FDR corrected).

We then tested our hypothesis and compare the FC between all the cortical ROIs in the three groups with ANOVA. False positive control in ROI-to-ROI analyses was performed using false discovery rate (FDR) correction for multiple comparisons (alpha-level = 0.05). We run separate post-hoc analyses with independent t-tests between groups for significant connections resulting from the ANOVA, correcting for the number of tests with FDR. All statistical analyses were also performed after regressing out the effect of migraine frequency, age, and sex.

2.7. Multinomial logistic regression

From both the cortico-cortical and the thalamo-cortical FC analysis we obtained a set of connections which were altered in AIWS with respect to HC and/or MA. In order to find the FC patterns which were most likely associated with AIWS, we entered the FC values of the altered connections in a multinomial logistic regression and performed model selection based on the Akaike's information criterion (AIC) (42). We started from a full model with formula GROUP ~ C_1 * C_2 *C_3 …*C_N, where GROUP was a dependent categorical variable (AIWS, MA or HC), and C_1 to C_N, were the individual FC values, used as explanatory variables.

To test the accuracy of the resulting model we split the patients in two partitions using even and odd IDs. We used the first partition to train the model and the second to test the accuracy of model predictions. We repeated the same procedure, using the second partition to train and the first partition to test the model. Then we calculated the average model accuracy as the average of the two estimates. We further calculated the area under the curve (AUC) of the receiver operating characteristic (ROC) curve to compare model accuracy in discriminating each pair of groups.

3. Results

3.1. Participants

Out of 40 patients with AIWS identified in the context of the cohort study on AIWS (6), 12 accepted to undergo an MRI and were therefore included in the present study. Twelve migraine patients with typical aura (MA) were also recruited among the 52 patients available from the same study. Typical aura was characterized by visual symptoms (including phosphenes, photopsia and visual blurring) or visual and somatosensory (paresthesia) symptoms. Four patients in the AIWS and three in the MA group received a diagnosis of chronic migraine, while all the remaining patients suffered from episodic migraine. All patients with AIWS also experienced typical visual aura associated with the migraine attack. A group of 24 sex- and age-matched healthy controls without any significant neurological or systemic disorders was blindly selected among those available from Human Neurosciences Department archive. T1-weighted images of the HC group were reviewed by a neurologist/neuroradiologist, to ascertain the absence of structural brain alterations.

Demographic and clinical information are provided in Table 1 and Supplementary Tables 1, 2. Patients did not significantly differ for any demographic characteristics.

3.2. Whole-brain thalamic functional connectivity

We found group differences in thalamic FC in four clusters (Figure 1). Thalamic nuclei were more connected with the anterior cingulate cortex (ACC: peak MNI coordinates: −2, 48, −2) in AIWS [$t(19.6)$: 3.8, $p < 0.01$] and in MA [$t(27.9)$: 2.5, $p = 0.017$] than in HC. This hyper-connectivity was significantly higher in AIWS than in MA [AIWS vs. MA: $t(20.5)$: 5.9].

We also found higher FC between thalamic nuclei and the anterior precuneus (AP: peak MNI coordinates: 54, −44, 2) in AIWS [$t(18.4)$: 5.4, $p < 0.01$] and MA [$t(22)$: 3.3, $p < 0.01$] than in HC, with a significantly higher FC in AIWS than in MA [$t(21)$: 2.3, $p = 0.03$].

The thalamic FC with the posterior precuneus (PP) and the calcarine region was higher in both AIWS [PP: $t(21.4)$: 5.8, $p < 0.01$; calcarine cortex: $t(20.7)$: 1.7, $p = 0.29$] and MA [PP: $t(21.5)$: 1.6, $p = 0.11$; calcarine cortex: $t(17.6)$: 4.6, $p < 0.01$] compared to HC. FC of these regions, however, was comparable between AIWS and MA [PP: $t(21.5)$: 1.6, $p = 0.11$; calcarine cortex: $t(14.9)$: 4.9, $p < 0.01$].

3.3. Cortico-cortical functional connectivity.

At the cortical level the ANOVA found a significant group effect in the FC between a region located in the left lateral occipital cortex (Lausanne atlas ID 214) and the ipsilateral posterior part of the superior temporal sulcus (Lausanne atlas ID 234), (Figure 2; ANOVA: $F = 19.7$, $p = 0.018$). This difference was due to higher FC between the two regions in AIWS than HC [$t(34)$: 5.6, $p < 0.01$] and MA [$t(22)$: 4.4, $p < 0.01$]. Conversely, HC and MA were not significantly different [HC vs. MA: $t(34)$: 0.03, $p = 0.97$]. Migraine frequency, age and sex showed no significant effect.

3.4. Multinomial logistic regression

In order to find the most relevant alterations characterizing AIWS with respect to HC and MA, we performed a multinomial logistic regression and performed model selection based on the AIC starting from a full model with formula: GROUP ~ $C_{V3\text{-}STS}$* $C_{Thal\text{-}ACC}$ *$C_{Thal\text{-}AP}$ *$C_{Thal\text{-}PP}$*$C_{Thal\text{-}Calcarine}$. The final model included only three main effects (i.e., FC between V3 and STS and thalamo-cortical FC with calcarine cortex and posterior precuneus) and had formula GROUP ~ $C_{V3\text{-}STS}$ + $C_{Thal\text{-}PP}$ + $C_{Thal\text{-}Calcarine}$ (Supplementary Table 3). The model predicted that for a 0.1 increase in FC between the thalamus and the posterior precuneus, or between the thalamus and the calcarine cortex, the probability of being a healthy individual as compared to AIWS fell dramatically (Thal-PP: OR = 0.008, $p = 0.02$; Thal-Calcarine cortex: OR = 0.003, $p = 0.047$). Moreover, a similar increase in the FC between area V3 and STS almost doubled the risk of experiencing AIWS episodes instead of a typical aura (OR 0.476, $p = 0.012$).

10.3389/fneur.2023.1210811

TABLE 1 Demographic and clinical information of the three groups.

N	Sex	Age	Age at onset	Headache frequency (days/month)	Duration of AIWS episodes	Description of AIWS symptoms	AIWS type
1	F	45–49	25–29	6	Up to 4 h	Macrosomatognosia of face and upper limbs, mosaic vision, derealization, depersonalization, slowing in the perception of time	Somatosensory + Visual (type C)
2	F	55–59	20–24	20	20–30 min	Micropsia, derealization, depersonalization, slowing in the perception of time	Visual (type B)
3	F	15–19	15–19	25	10 min	Macropsia, telopsia, derealization, depersonalization, slowing in the perception of time	Visual (type B)
4	F	45–49	5–9	2	15 min	Microsomatognosia, telopsia, pelopsia, derealization, depersonalization	Somatosensory + Visual (type C)
5	M	25–29	10–14	8	Up to 1 h	Telopsia, pelopsia, mosaic vision, slowing in the perception of time	Visual (type B)
6	F	45–49	15–19	5	Not reported	Macrosomatognosia of hands, micropsia, macropsia, telopsia, pelopsia, derealization, depersonalization, slowing in the perception of time	Somatosensory + Visual (type C)
7	M	35–39	20–24	10	Not reported	Micropsia	Visual (type B)
8	F	55–59	15–19	2	Up to 1 h	Micropsia, macropsia, derealization	Visual (type B)
9	F	40–44	10–14	10	30 min	Macrosomatognosia left hemiface, macropsia, pelopsia	Somatosensory + Visual (type C)
10	F	45–49	45–49	3	30 min	Macrosomatognosia of hands and upper limbs, aschematia, macropsia, telopsia, mosaic vision, derealization, depersonalization, slowing in the perception of time	Somatosensory + Visual (type C)
11	F	25–29	10–14	3	1 h	Aschematia, mosaic vision, derealization, depersonalization, slowing in the perception of time	Visual (type B)
12	M	40–49	25–29	4	Not reported	Pelopsia, mosaic vision, loss of stereotactic vision, slowing in the perception of time	Visual (type B)

Mean and standard deviation and frequency counts (percentage) are reported. AIWS, Alice in Wonderland Syndrome; MA, migraine with aura; HC, healthy controls.

The accuracy of the model in discriminating the patients belonging to the AIWS, MA and HC group was 83.06%. We also calculated the AUC of the ROC curve (Figure 3A), which was above 0.8 for all the pairs of groups ($AUC_{AIWSvsHC:}$ 0.95; $AUC_{AIWSvsMA}$: 0.86; AUC_{HCvsMA}: 0.84).

Thus, the strength of FC between the thalamus and the posterior precuneus, between the thalamus and the calcarine cortex and between V3 and STS was able to discriminate the three groups with a high level of confidence. In addition, alterations in the FC between the thalamus and posterior precuneus and calcarine regions were mostly relevant in discriminating both groups of patients with migraine from HC and did not characterize AIWS (see also Figure 3B). Conversely, the hyper-connectivity between V3 and STS resulted to be distinctive of AIWS, since it mainly contributed to discriminating between patients with migraine and AIWS from those with simple aura and healthy individuals.

4. Discussion

The present study provides novel evidence of interictal alterations in brain functional connectivity in patients with migraine with aura related AIWS. We found cortico-cortical FC alterations, which are distinctive of AIWS, both compared to HC and patients with migraine with typical aura, likely representing a neuroimaging correlate of the syndrome in this population. Conversely, thalamo FC alterations seemed to be more related to migraine aura regardless of AIWS symptoms. Both AIWS and MA showed enhanced FC between the thalamus and four cortical regions, namely the anterior cingulate, anterior and posterior precuneus and calcarine cortex, with respect to HC. The increased FC between the thalamus and precuneus and calcarine regions was comparable between patients with AIWS and those with typical aura, thus representing a trait mainly related to migraine with aura. The increased FC between the thalamus and anterior precuneus and ACC was more marked in patients with AIWS than in patients with typical aura, likely because of more complex visual and somatosensory symptoms in AIWS than in MA patients. In summary, none of the alterations in thalamocortical FC seems to be specifically related to AIWS, suggesting that to some extent MA and AIWS could represent a clinical continuum, and that similar pattern of FC alterations could be the common predisposing factor.

On the other hand, alterations in cortico-cortical FC appear to be specific of the AIWS. Indeed, whole brain ROI-to-ROI analysis showed an increased interictal FC between the lateral occipital cortex (V3) and the posterior STS, a part of the temporo-parietal junction (TPJ), in patients with AIWS, with respect to both MA and HC. This result may represent a neuroimaging marker of AIWS in migraineurs,

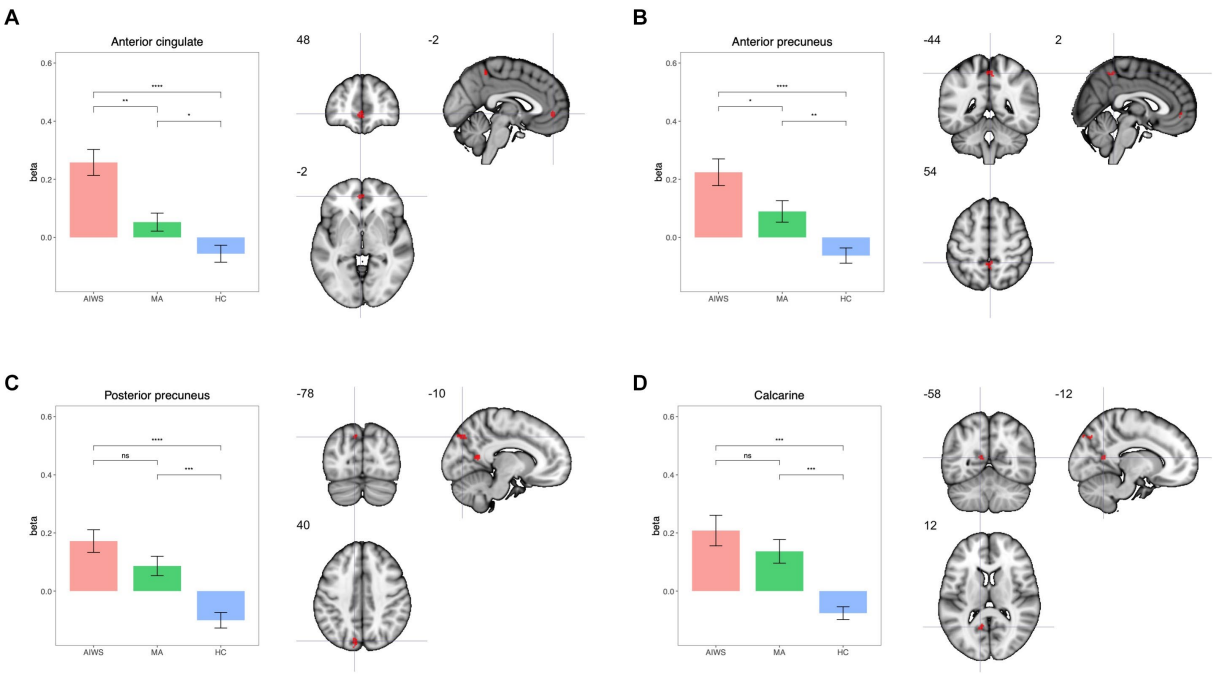

FIGURE 1
Results of the seed-to-voxel thalamo-cortical connectivity analysis. Sub-plots showing on left the mean beta values for connectivity in each group and on the right brain maps with MNI coordinates for each significant cluster: **(A)** anterior cingulate cortex, **(B)** anterior precuneus; **(C)** posterior precuneus; **(D)** calcarine.

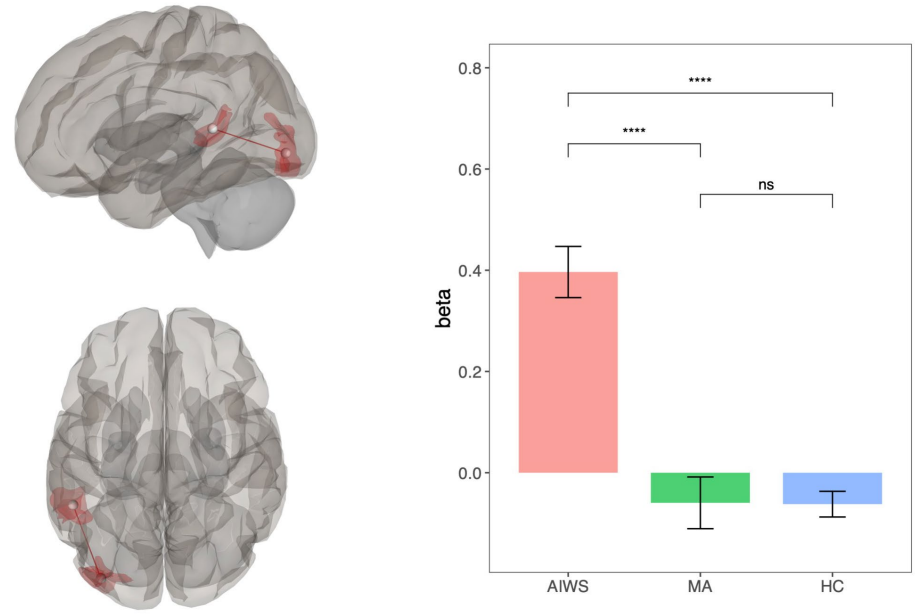

FIGURE 2
Results of the ROI-to-ROI whole brain connectivity analysis. On the right, brain maps showing the statistically significant connection between left lateral occipital cortex and left superior temporal sulcus; on the left, bar-plots with mean connectivity values for each group.

suggesting that the occurrence of AIWS episodes in this population, rather than other aura types, may be associated with this specific FC pattern. It is important to stress that we included patients with only visual AIWS disturbance as well as patients with visual and somatosensory disturbance. This decision was due to the fact that epidemiologically in the age interval we consider the occurrence of visual, somatosensory and combined forms are mostly identical (10), suggesting a shared mechanism.

10.3389/fneur.2023.1210811

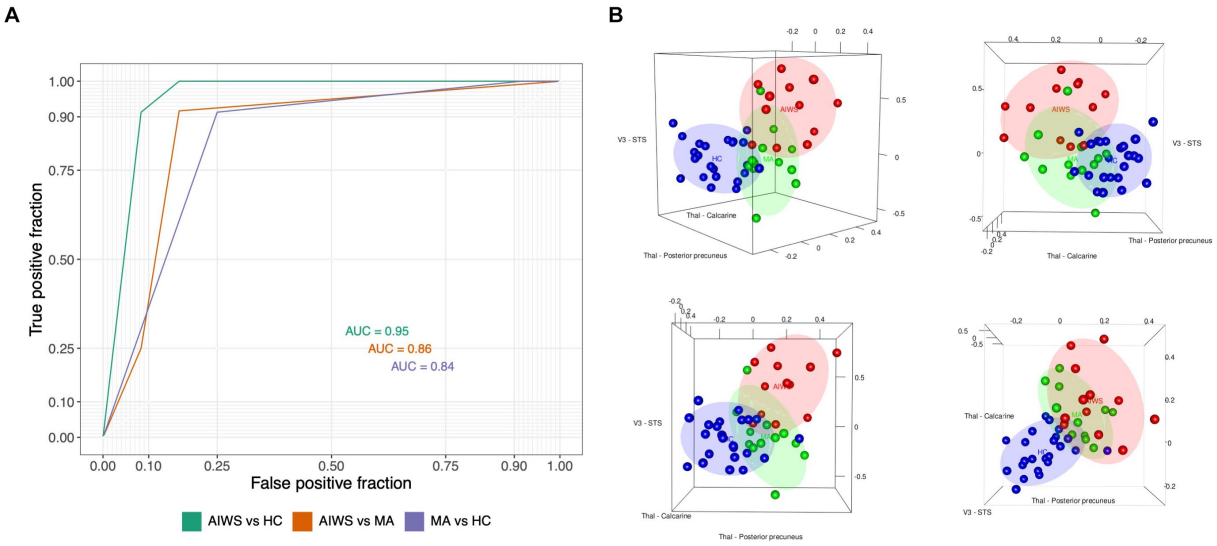

FIGURE 3
Results of the Multinomial logistic regression and the Receive Operating Characteristic Curve (ROC) analyses. **(A)** receiver operating characteristic curve (ROC) for prediction of AIWS diagnosis based on the connections selected with a multinomial logistic regression (i.e., V3 to STS connectivity and thalamocortical connectivity with calcarine and posterior precuneus). AUC, Area under the curve. **(B)** The 3D scatterplots report, on each of the axis, the connectivity values of the three connections which were mostly relevant for the discrimination of AIWS (red), MA (green), and healthy control (blue). The connectivity between the thalamus and the posterior precuneus and between the thalamus and the calcarine region was more informative about the diagnosis of migraine, regardless of AIWS, with respect to healthy controls (bottom right plot). The V3-STS connectivity is more specifically related to the AIWS.

Interestingly, the identified occipital region corresponds to the V3 area, which has been implicated in cortical spreading depression (CSD) due to an increase in BOLD activity time-locked to the onset of aura symptoms (43). A recent study also showed that V3 is the central region of a wide brain network of areas characterized by volume loss in migraineurs (44), suggesting a relationship between the pattern of FC of V3 and wide-spread structural brain alterations in migraine. The posterior part of the STS is an associative area implicated in multisensory integration (45), where populations of bimodal and trimodal neurons combine auditory, visual, tactile and vestibular inputs (45, 46), thus contributing to the mapping of exteroceptive stimuli in the external environment and with respect to the body (46). The involvement of the posterior STS is therefore consistent with the clinical manifestation of AIWS, which is characterized by the misperception of the distance and size of external objects and parts of one's own body.

While the fMRI analyses employed do not directly provide information about the directionality of this increased connectivity between V3 and STS, our results provide some insights into the potential mechanisms underpinning AIWS symptoms. A first hypothesis is that AIWS symptoms might be caused by a diaschisis-like phenomenon: a change of function in a portion of the brain connected to a distant, but impaired, brain area. In patients with AIWS, a sudden deactivation of V3, induced by the CSD during the ictal phase, might cause an impairment in STS activity due to their increased inter-ictal functional connectivity. Alternatively, this enhanced FC may increase the likelihood of the CSD to propagate to the STS, directly impacting on STS functionality. A third possibility is that the complexity of AIWS clinical presentation (i.e., the combination of different perceptual disturbances also associated to cognitive alterations) could be attributed to an abnormal, over-compensatory modulation exerted by the STS on lower-level areas, as V3, due to a deteriorated sensory inflow.

An important limitation of our study is the relatively small sample size. This limitation is partially compensated by the fact that our groups are relatively homogeneous. Moreover, we conducted data-driven whole brain analyses applying conservative corrections for multiple comparisons. Another limitation is that we could not stratify the patients with AIWS according to their specific symptoms. Thus, we could not identify alterations specific to AIWS subtypes (10), although, at present, there is no evidence supporting the idea that different subtypes of the syndrome might be caused by different neuropathological mechanisms. For similar reasons, we were not able to compare AIWS with MA patients with different levels of complexity of migraine aura, which is an important factor associated to different functional connectivity abnormalities (47, 48). Future studies with larger sample size may address these relevant questions. Additionally, other types of fMRI analysis that allow to discriminate between patients with and without MA, such as wavelet decomposition analysis (49), might to contribute to further reveal important pathophysiological mechanisms in AIWS.

In conclusion, we found common and distinct alterations in functional connectivity in patients with migraine experiencing AIWS episodes and patients with typical aura during the interictal phase. We found that patients with MA and AIWS share similar alterations in thalamic FC, suggesting that these alterations are not specific of AIWS. Conversely, hyper-connectivity between V3 and the posterior STS, characterized only migraineurs with AIWS, likely representing a specific feature of AIWS in these patients. These findings are consistent with the hypothesis that AIWS might be caused by an altered FC between sensory and multisensory associative areas. Our study provides a working hypothesis for studying the pathophysiological mechanisms underlying the occurrence of AIWS episodes in patients

with AIWS attributable to other etiologies than migraine, which could verify the generalizability of this hypothesis.

Data availability statement

The dataset presented in this article are not readily available because of patients confidentiality and participants privacy restrictions. Requests to access the raw datasets should be directed to the corresponding author.

Ethics statement

The studies involving human participants were reviewed and approved by Ethics committee of Policlinico Umberto I. The patients/participants provided their written informed consent to participate in this study.

Author contributions

GM, VM, AV, CP, NP, MP, CG, PP, and VP: ideation, data collection, data analysis, interpretation, and drafting the manuscript. All authors contributed to the article and approved the submitted version.

Funding

Open access funding by University of Geneva.

Acknowledgments

The authors would like to thank both reviewers for their helpful insight in the production of this paper. In particular, one of the reviewers helped in defining the interpretative key of the functional connectivity results.

Conflict of interest

The authors declare that the research was conducted in the absence of any commercial or financial relationships that could be construed as a potential conflict of interest.

Publisher's note

All claims expressed in this article are solely those of the authors and do not necessarily represent those of their affiliated organizations, or those of the publisher, the editors and the reviewers. Any product that may be evaluated in this article, or claim that may be made by its manufacturer, is not guaranteed or endorsed by the publisher.

Supplementary material

The Supplementary material for this article can be found online at: https://www.frontiersin.org/articles/10.3389/fneur.2023.1210811/full#supplementary-material

References

1. Vos T, Abajobir AA, Abbafati C, Abbas KM, Abate KH, Abd-Allah F, et al. Global, regional, and national incidence, prevalence, and years lived with disability for 328 diseases and injuries for 195 countries, 1990-2016: a systematic analysis for the global burden of disease study 2016. *Lancet*. (2017) 390:1211–59. doi: 10.1016/S0140-6736(17)32154-2

2. Stovner LJ, Nichols E, Steiner TJ, Abd-Allah F, Abdelalim A, Al-Raddadi RM, et al. Global, regional, and national burden of migraine and tension-type headache, 1990–2016: a systematic analysis for the global burden of disease study 2016. *Lancet Neurol*. (2018) 17:954–76. doi: 10.1016/S1474-4422(18)30322-3

3. Charles AC, Baca SM. Cortical spreading depression and migraine. *Nat Rev Neurol*. (2013) 9:637–44. doi: 10.1038/nrneurol.2013.192

4. Dooley JM, Augustine HF, Gordon KE, Brna PM, Westby E. Alice in Wonderland and other migraine associated phenomena—evolution over 30 years after headache diagnosis. *Pediatr Neurol*. (2014) 51:321–3. doi: 10.1016/j.pediatrneurol.2014.05.032

5. Valença MM, De Oliveira DA, Martins HADL. Alice in Wonderland syndrome, burning mouth syndrome, cold stimulus headache, and HaNDL: narrative review. *Headache*. (2015) 55:1233–48. doi: 10.1111/head.12688

6. Mastria G, Mancini V, Di CM, Puma M, Alessiani M, Petolicchio B, et al. Prevalence and characteristics of Alice in Wonderland syndrome in adult migraineurs: perspectives from a tertiary referral headache unit. *Cephalalgia*. (2020) 41:515–24. doi: 10.1177/0333102420968245

7. Beh SC, Masrour S, Smith SV, Friedman DI. Clinical characteristics of Alice in Wonderland syndrome in a cohort with vestibular migraine. *Neurol Clin Pract*. (2018) 8:389–96. doi: 10.1212/CPJ.0000000000000518

8. Mastria G, Mancini V, Viganò A, Di Piero V. Alice in Wonderland syndrome: a clinical and pathophysiological review. *Biomed Res Int*. (2016) 2016:1–10. doi: 10.1155/2016/8243145

9. Todd J. The syndrome of Alice in Wonderland. *Can Med J*. (1955) 73:701–4.

10. Lanska JR, Lanska DJ. Alice in Wonderland syndrome: Somesthetic vs visual perceptual disturbance. *Neurology*. (2013) 80:1262–4. doi: 10.1212/WNL.0b013e31828970ae

11. O'Toole P, Modestino EJ. Alice in Wonderland syndrome: a real life version of Lewis Carroll's novel. *Brain Dev*. (2017) 39:470–4. doi: 10.1016/j.braindev.2017.01.004

12. Cinbis M, Aysun S. Alice in Wonderland syndrome as an initial manifestation of Epstein-Barr virus infection. *Br J Ophthalmol*. (1992) 76:316. doi: 10.1136/bjo.76.5.316

13. García-Cabo C, Fernández-Domínguez J, García-Rodríguez R, Mateos Marcos V. Alice in Wonderland syndrome as the initial and sole manifestation of ischaemic stroke. *Neurologia*. (2019) 34:487–8. doi: 10.1016/j.nrl.2016.10.011

14. ElTarhouni AH, Beer L, Mouthon M, Erni B, Aellen J, Annoni JM, et al. The right thalamic ventral posterolateral nucleus seems to be determinant for macrosomatognosia: a case report. *BMC Neurol*. (2020) 20:1–9. doi: 10.1186/s12883-020-01970-3

15. Mastria G, Mancini V, Viganò A, De Sanctis R, Letteri F, Toscano M, et al. Temporal–occipital glioblastoma presenting with Alice in Wonderland syndrome in a patient with a long-time history of migraine without aura. *Neurocase*. (2018) 24:242–4. doi: 10.1080/13554794.2018.1562079

16. Morland D, Wolff V, Dietemann JL, Marescaux C, Namer IJ. Robin Hood caught in Wonderland: brain SPECT findings. *Clin Nucl Med*. (2013) 38:979–81. doi: 10.1097/RLU.0000000000000230

17. Brumm K, Walenski M, Haist F, Robbins SL, Granet DB, Love T. Functional magnetic resonance imaging of a child with alice in Wonderland syndrome during an episode of micropsia. *J AAPOS*. (2010) 14:317–22. doi: 10.1016/j.jaapos.2010.03.007

18. Gencoglu EA, Alehan F, Erol I, Koyuncu A, Aras M. Brain SPECT findings in a patient with Alice in Wonderland syndrome. *Clin Nucl Med*. (2005) 30:758–9. doi: 10.1097/01.rlu.0000182278.13389.a3

19. Mancini V, Mastria G, Frantellizzi V, Viganò A, Petsas N, Sollaku S, et al. Aripiprazole-triggered Alice in Wonderland syndrome episodes studied with 99mTc-HMPAO brain SPECT. *Eur Neurol*. (2018) 79:333–4. doi: 10.1159/000490902

20. Yokoyama T, Okamura T, Takahashi M, Momose T, Kondo S. A case of recurrent depressive disorder presenting with Alice in Wonderland syndrome: psychopathology and pre- and post-treatment FDG-PET findings. *BMC Psychiatry*. (2017) 17:4–9. doi: 10.1186/s12888-017-1314-2

21. Piervincenzi C, Petsas N, Viganò A, Mancini V, Mastria G, Puma M, et al. Functional connectivity alterations in migraineurs with Alice in Wonderland syndrome. *Neurol Sci*. (2023) 44:305–17. doi: 10.1007/s10072-022-06404-1

22. Azimova J, Sergeev A, Skorobogatykh K, Klimov E, Tabeeva G, Rachin A. Alice-in-Wonderland syndrome in patients with migraine. *Br J Med Med Res*. (2016) 13:1–11. doi: 10.9734/BJMMR/2016/23997

23. Petrušić I, Zidverc-Trajković J. Redefining types of migraine aura. *Cephalalgia*. (2021) 41:274–5. doi: 10.1177/0333102420970186

24. Ashina S, Bentivegna E, Martelletti P, Eikermann-Haerter K. Structural and functional brain changes in migraine. *Pain Ther*. (2021) 10:211–23. doi: 10.1007/s40122-021-00240-5

25. Puledda F, Ffytche D, O'Daly O, Goadsby PJ. Imaging the visual network in the migraine Spectrum. *Front Neurol*. (2019) 10:1–12. doi: 10.3389/fneur.2019.01325

26. Skorobogatykh K, van Hoogstraten WS, Degan D, Prischepa A, Savitskaya A, Ileen BM, et al. Functional connectivity studies in migraine: what have we learned? *J Headache Pain*. (2019) 20:108. doi: 10.1186/s10194-019-1047-3

27. Chong CD, Schwedt TJ, Hougaard A. Brain functional connectivity in headache disorders: a narrative review of MRI investigations. *J Cereb Blood Flow Metab*. (2019) 39:650–69. doi: 10.1177/0271678X17740794

28. Coppola G, Di Renzo A, Tinelli E, Petolicchio B, Parisi V, Serrao M, et al. Thalamo-cortical networks in subtypes of migraine with aura patients. *J Headache Pain*. (2021) 22:1–10. doi: 10.1186/s10194-021-01272-0

29. Wang T, Chen N, Zhan W, Liu J, Zhang J, Liu Q, et al. Altered effective connectivity of posterior thalamus in migraine with cutaneous allodynia: a resting-state fMRI study with granger causality analysis. *J Headache Pain*. (2016) 17:1–11. doi: 10.1186/s10194-016-0610-4

30. Tu Y, Fu Z, Zeng F, Maleki N, Lan L, Li Z, et al. Abnormal thalamocortical network dynamics in migraine. *Neurology*. (2019) 92:E2706–16. doi: 10.1212/WNL.0000000000007607

31. Qin ZX, Su JJ, He XW, Zhu Q, Cui YY, Zhang JL, et al. Altered resting-state functional connectivity between subregions in the thalamus and cortex in migraine without aura. *Eur J Neurol*. (2020) 27:2233–41. doi: 10.1111/ene.14411

32. Hansen JM, Baca SM, VanValkenburgh P, Charles A. Distinctive anatomical and physiological features of migraine aura revealed by 18 years of recording. *Brain*. (2013) 136:3589–95. doi: 10.1093/brain/awt309

33. Tourbier S, Aleman-Gomez Y, Mullier E, Griffa A, Bach Cuadra MHP. *Connectomicslab/connectomemapper3: connectome mapper v3.0.0-RC4 (version v3.0.0-RC4)* Zenodo (2020).

34. Desikan RS, Se F, Fischl B, Quinn BT, Dickerson BC, Blacker D, et al. An automated labeling system for subdividing the human cerebral cortex on MRI scans into gyral based regions of interest. *Neuro Image*. (2006) 31:968–80. doi: 10.1016/j.neuroimage.2006.01.021

35. Cammoun L, Gigandet X, Meskaldji D, Thiran JP, Sporns O, Do KQ, et al. Mapping the human connectome at multiple scales with diffusion spectrum MRI. *J Neurosci Methods*. (2012) 203:386–97. doi: 10.1016/j.jneumeth.2011.09.031

36. Ashburner J, Friston KJ. Unified segmentation. *NeuroImage*. (2005) 26:839–51. doi: 10.1016/j.neuroimage.2005.02.018

37. Whitfield-gabrieli S, Nieto-castanon A. Conn: a functional connectivity toolbox for correlated and Anticorrelated brain networks. *Brain Connect*. (2012) 2:125–41. doi: 10.1089/brain.2012.0073

38. Tousignant B, Eugène F, Sirois K, Jackson PL. Difference in neural response to social exclusion observation and subsequent altruism between adolescents and adults. *Neuropsychologia*. (2018) 116:15–25. doi: 10.1016/j.neuropsychologia.2017.04.017

39. Behzadi Y, Restom K, Liau J, Liu TT. A component based noise correction method (CompCor) for BOLD and perfusion based fMRI. *Hum Brain Mapp J*. (2007) 37:90–101. doi: 10.1016/j.neuroimage.2007.04.042

40. Hrybouski S, Aghamohammadi-sereshki A, Madan CR, Shafer AT, Baron CA, Seres P, et al. Amygdala subnuclei response and connectivity during emotional processing. *NeuroImage*. (2016) 133:98–110. doi: 10.1016/j.neuroimage.2016.02.056

41. Mancini V, Zöller D, Schneider M, Schaer M, Eliez S. Abnormal development and Dysconnectivity of distinct thalamic nuclei in patients with 22q11.2 deletion syndrome experiencing auditory hallucinations. *Biol Psychiatry Cogn Neurosci Neuroimaging*. (2020) 5:875–90. doi: 10.1016/j.bpsc.2020.04.015

42. Akaike H. Canonical correlation analysis of time series and the use of an information criterion. *Math Sci Eng*. (1976) 126:27–96. doi: 10.1016/S0076-5392(08)60869-3

43. Hadjikhani N, Sanchez Del Rio M, Wu O, Schwartz D, Bakker D, Fischl B, et al. Mechanisms of migraine aura revealed by functional MRI in human visual cortex. *Proc Natl Acad Sci U S A*. (2001) 98:4687–92. doi: 10.1073/pnas.071582498

44. Burke MJ, Joutsa J, Cohen AL, Soussand L, Cooke D, Burstein R, et al. Mapping migraine to a common brain network. *Brain*. (2020) 143:541–53. doi: 10.1093/brain/awz405

45. Stein BE, Stanford TR. Multisensory integration: current issues from the perspective of the single neuron. *Nat Rev Neurosci*. (2008) 9:255–66. doi: 10.1038/nrn2331

46. Blanke O, Slater M, Serino A. Behavioral, neural, and computational principles of bodily self-consciousness. *Neuron*. (2015) 88:145–66. doi: 10.1016/j.neuron.2015.09.029

47. Petrusic I, Viana M, Dakovic M, Zidverc-Trajkovic J. Application of the migraine Aura complexity score (MACS): clinical and neuroimaging study. *Front Neurol*. (2019) 10:1112. doi: 10.3389/fneur.2019.01112

48. Silvestro M, Tessitore A, Di Nardo F, Scotto di Clemente F, Trojsi F, Cirillo M, et al. Functional connectivity changes in complex migraine aura: beyond the visual network. *Eur J Neurol*. (2022) 29:295–304. doi: 10.1111/ene.15061

49. Faragó P, Tuka B, Tóth E, Szabó N, Király A, Csete G, et al. Interictal brain activity differs in migraine with and without aura: resting state fMRI study. *J Headache Pain*. (2017) 18:8. doi: 10.1186/s10194-016-0716-8